energy harbor

Energy Harbor Nuclear Corp.
Perry Nuclear Power Plant
10 Center Road
P.O. Box 97
Perry, Ohio 44081

Rod L. Penfield
Site Vice President, Perry Nuclear

440-280-5382

July 14, 2022
L-22-171

10 CFR 50.55a

ATTN: Document Control Desk
U.S. Nuclear Regulatory Commission
Washington, DC 20555-0001

Subject:
Perry Nuclear Power Plant
Docket No. 50-440, License No. NPF-58
Response to Request for Additional Information Regarding Proposed Inservice Inspection Alternative IR-063 (EPID L-2022-LLR-0005)

By letter dated January 5, 2022, (Agencywide Documents and Access Management System (ADAMS) Accession No. ML22006A167), Energy Harbor Nuclear Corp. requested Nuclear Regulatory Commission (NRC) staff approval of a proposed inservice inspection alternative (IR-063) to the American Society of Mechanical Engineers (ASME) Boiler and Pressure Vessel Code (ASME Code), Section XI, Table IWB-2500-1, "Examination Category B-D, Full Penetration Welded Nozzles in Vessels," for use at Perry Nuclear Power Plant (PNPP). The IR-063 request proposed alternative inservice inspection requirements for the volumetric inspection of the PNPP reactor feedwater nozzles from those required for the nozzles in the ASME Code, Section XI, Table IWB-2500-1, Examination Category B-D, Inspection items B3.90, "Nozzle-to-Vessel Welds," and B3.100, "Nozzle Inside Radius Section." By electronic mail dated May 16, 2022, the NRC staff requested additional information to complete its review of the proposed alternative. The requested information is attached.

There are no regulatory commitments contained in this submittal. If there are any questions or if additional information is required, please contact Mr. Phil H. Lashley, Manager - Fleet Licensing, at (330) 696-7208.

Sincerely,

Rod L. Penfield

Attachment: Response to Request for Additional Information

cc: NRC Region III Administrator
NRC Resident Inspector
NRC Project Manager

By letter dated January 5, 2022, (ADAMS Accession No. ML22006A167), Energy Harbor Nuclear Corp. submitted a proposed inservice inspection (ISI) alternative, IR-063, for use at Perry Nuclear Power Plant (PNPP). In IR-063, Energy Harbor Nuclear Corp. proposed alternative ISI requirements for the volumetric inspection of the PNPP reactor feedwater (RFW) nozzles from those required for the nozzles in the American Society of Mechanical Engineers (ASME) Boiler and Pressure Vessel Code (ASME Code), Section XI, Table IWB-2500-1, Examination Category B-D, "Full Penetration Welded Nozzles in Vessels," Inspection items B3.90, "Nozzle-to-Vessel Welds," and B3.100, "Nozzle Inside Radius Section." By electronic mail dated May 16, 2022, the Nuclear Regulatory Commission (NRC) staff requested additional information to complete its review of the proposed alternative. The NRC staff's request is presented in bold type, followed by the Energy Harbor Nuclear Corp. response.

(IR-063) RAI-NVIB-01

For assessed RFW nozzle-to-vessel welds, clarify how the VIPERNOZ PFM [probabilistic fracture mechanics] crack growth methods model the impacts of postulated cracks in the inaccessible regions (i.e., un-inspected regions) of the referenced weld locations (i.e., for RFW Nozzle Weld ID Nos. 1B13-N4A-KA thru 1B13-N4F-KA).

Response:

The algorithm used by VIPERNOZ in the handling of inspected percentage of weld length/volume is by a random number to identify whether an individual crack is in the inspection percentage. If the random number is less than the inspection percentage (that is, within the inspection region), the crack is inspected. For each inservice inspection, a different random number is used for each crack to simulate that a different weld region could be inspected each time. If the random number is greater than the inspection percentage, no inspection is performed, and the crack continues to grow. If the random number is less than the inspection percentage resulting in inspection, the probability of detection (POD) curve is applied. If detected, a flaw is assumed to be repaired or properly dispositioned, and thus, cannot cause failure; if not detected, the flaw continues to grow, and thus, can lead to failure.

Specifically, the PFM analysis in Section 3.2.4 of Structural Integrity Associates, Inc. (SIA) Calculation Package No. 2001178.302 conservatively accounted for the most limiting 82.7 percent inspection coverage for the RFW nozzle-to-shell welds as follows:

For the first 30 years of inspection, the PFM analysis evaluated the following total inspection volume of all six RFW nozzles:

82.7% limiting coverage x 6/6 nozzles inspected = 82.7% total inspection volume

For the fourth and subsequent ISI intervals, the total inspection volume based on inspecting two of the six RFW nozzles is calculated as:

82.7% limiting coverage x 2/6 nozzles inspected = 27.6% total inspection volume

Following the technical bases in Electrical Power Research Institute (EPRI) Technical Reports BWRVIP-108-A, "Technical Basis for the Reduction of Inspection Requirements for the Boiling Water Reactor Nozzle-to-Vessel Shell Welds and Nozzle Inner Radii," and BWRVIP-241-A, "Probabilistic Fracture Mechanics Evaluation for the Boiling Water Reactor Nozzle-to-Vessel Shell Welds and Nozzle Blend Radii," the PFM analysis for the fourth and subsequent ISI intervals evaluated a total inspection volume of 25 percent, which is conservative relative to the calculated 27.6 percent that will be inspected in the fourth and subsequent ISI intervals.

(IR-063) RAI-NVIB-02

Justify the basis for the difference in the number of analyzed stress paths that were previously analyzed for the VIPERNOZ Monte Carlo runs of the CGS [Columbia Generating Station] RFW nozzle components versus the number of stress paths (i.e., the four stress paths P1 – P4) that have been analyzed for the PNPP RFW nozzle components in RR# [Relief Request Number] IR-063. As part of this justification, please explain:

(a) similarities and differences between the assumed stress types (i.e., hoop or axial) for stress paths P1 and P2 being applied to the PNPP RFW nozzle inside radius sections, as analyzed using the reiterative VIPERNOZ Monte Carlo runs for random generated inside radius semi-elliptical flaws in the radius sections;

Response to Part (a):

Figure 2 (Through-wall Stress Distributions, Unit Pressure), Figure 3 (Through-wall Stress Distributions, Nozzle Unit Moment Load), and Figure 4 (Through-wall Stress Distributions, Three Most Severe Thermal Transients) of the SIA Calculation Package No. 2001178.302, shows the comparison of the crack driving stress through-wall distribution for the blend radius region. The following three figures provide the data from Figure 2, Figure 3, and Figure 4 of SIA Calculation Package No. 2001178.302 specific to paths P1 and P2. The similarities between P1 and P3 are that the stresses that were generated are in hoop direction relative to the nozzle axis and perpendicular to the cutting-planes of the finite element model (FEM) and the nozzle inside blend radius is not cladded, thus there are no cladding stresses applied to P1 and P2.

Under internal pressure load, the stress distribution of P1 is higher as compared to P2, as displayed in Figure RAI-NVIB-02-A-1.

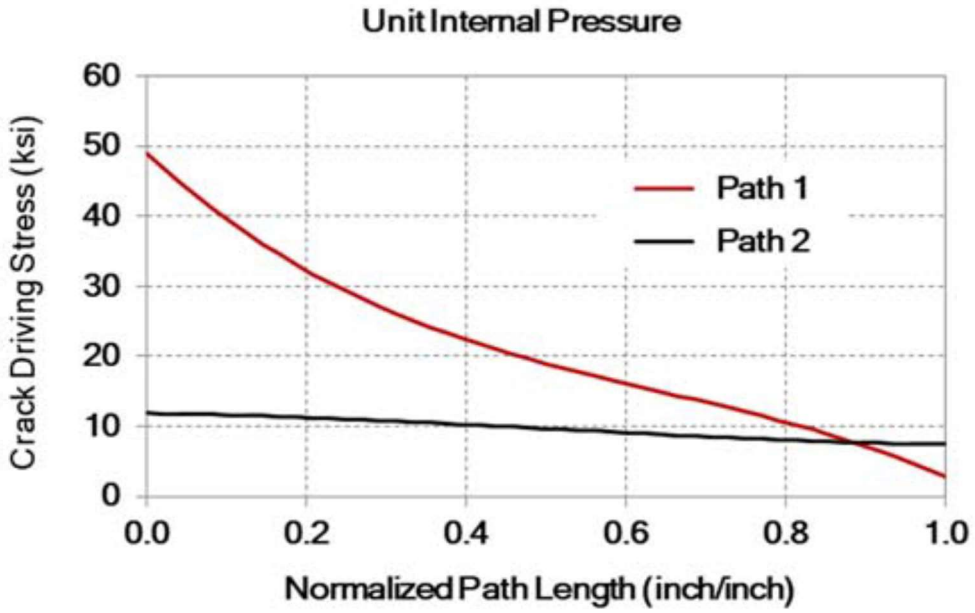

Figure RAI-NVIB-02-A-1: Unit Internal Pressure, Paths P1 and P2

Under mechanical piping moment loading, the difference between the through-wall stress distributions between P1 and P2 is negligible, as displayed in Figure RAI-NVIB-02-A-2.

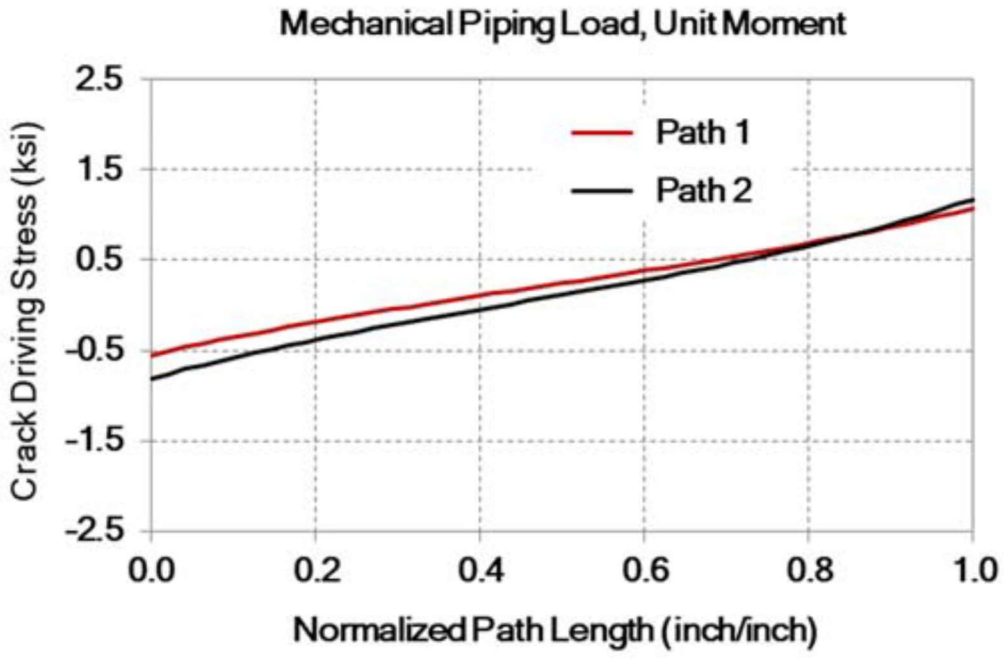

Figure RAI-NVIB-02-A-2: Mechanical Piping Load, Unit Moment Paths P1 and P2

Under the most severe thermal transient (Composite Loss of Feedwater Pumps Event), the difference between the through-wall stress distributions between P1 and P2 is negligible, as displayed in Figure RAI-NVIB-02-A-3.

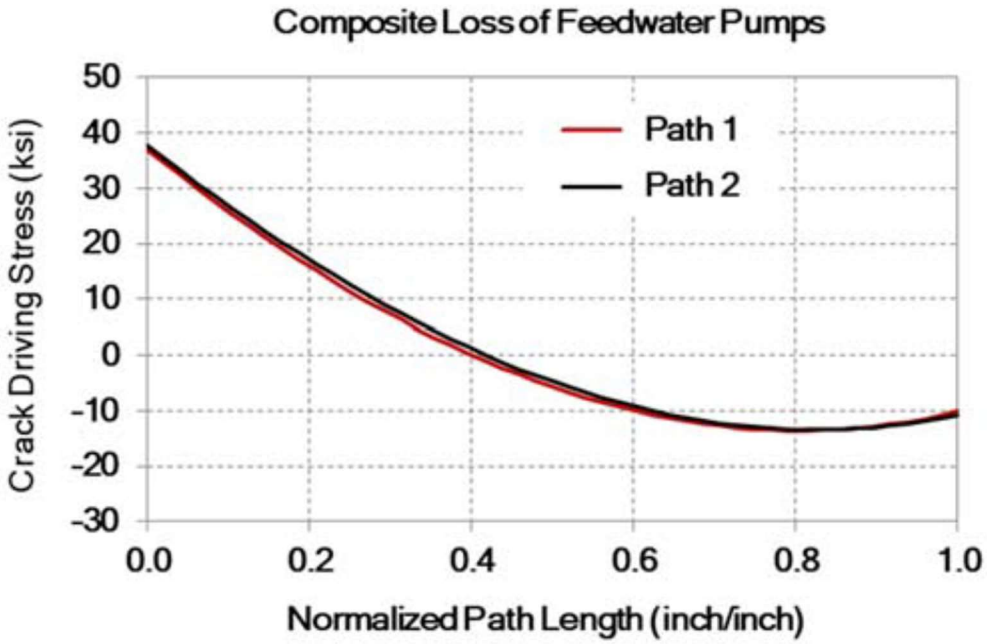

Figure RAI-NVIB-02-A-3: Composite Loss of Feedwater Pumps Paths P1 and P2

(b) which orientation of semi-elliptical flaw is being applied to stress paths P3 and P4 for the VIPERNOZ RFW nozzle-to-vessel weld assessments at PNPP;

Response to Part (b):

A semi-elliptical axial flaw was used for stress path P3 (hoop stress relative to the reactor pressure vessel (RPV) axis) and a semi-elliptical circumferential flaw was used for stress path P4 (axial stress relative to the RPV axis).

(c) the similarities and differences between the assumed stress type (i.e., hoop or axial stress) being applied to the VIPERNOZ Monte Carlo runs for PNPP RFW nozzle-to-vessel weld semi-elliptical axial flaws and semi-elliptical circumferential flaws (under the applicable stress path, P3 or P4, for the specified flaw type, including all applicable stress inputs).

Response to Part (c):

Figure 2 (Through-wall Stress Distributions, Unit Pressure), Figure 3 (Through-wall Stress Distributions, Nozzle Unit Moment Load), and Figure 4 (Through-wall Stress Distributions, Three Most Severe Thermal Transients) of the SIA Calculation Package No. 2001178.302, shows the comparison of the crack driving stress through-wall distribution for the nozzle-to-vessel weld region. The following three figures provide the data from Figure 2, Figure 3, and Figure 4 of SIA Calculation Package No. 2001178.302 specific to paths P3 and P4. P3 is generated as hoop stress relative to the RPV axis while P4 is generated as axial stress relative to the RPV axis.

Under internal pressure load, the stress distribution of P3 is higher as compared to P4, as displayed in Figure RAI-NVIB-02-C-1.

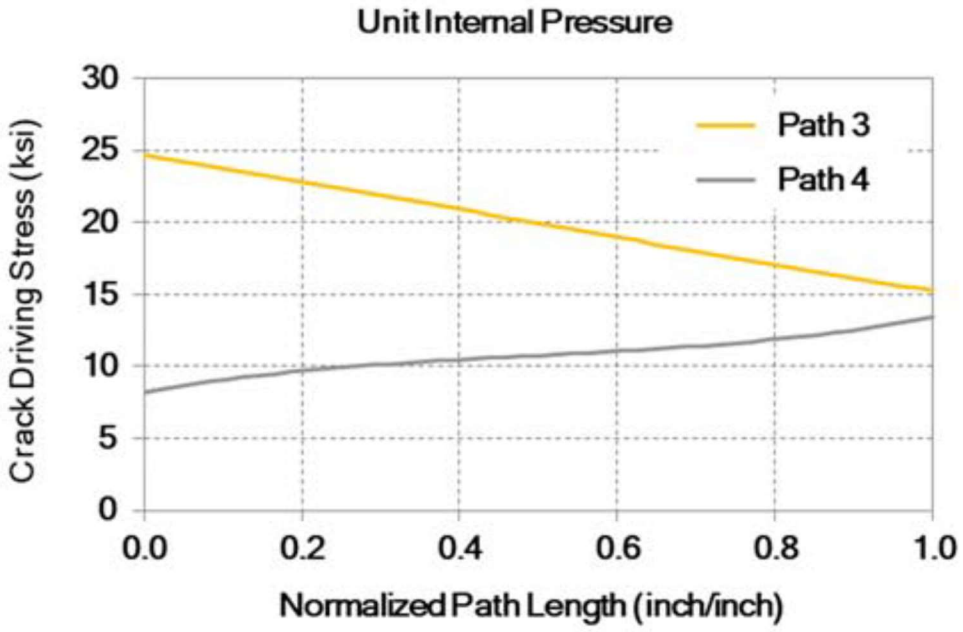

Figure RAI-NVIB-02-C-1: Unit Internal Pressure, Paths P3 and P4

Under mechanical piping moment loading, the difference between the through-wall stress distributions between P3 and P4 is negligible, as displayed in Figure RAI-NVIB-02-C-2.

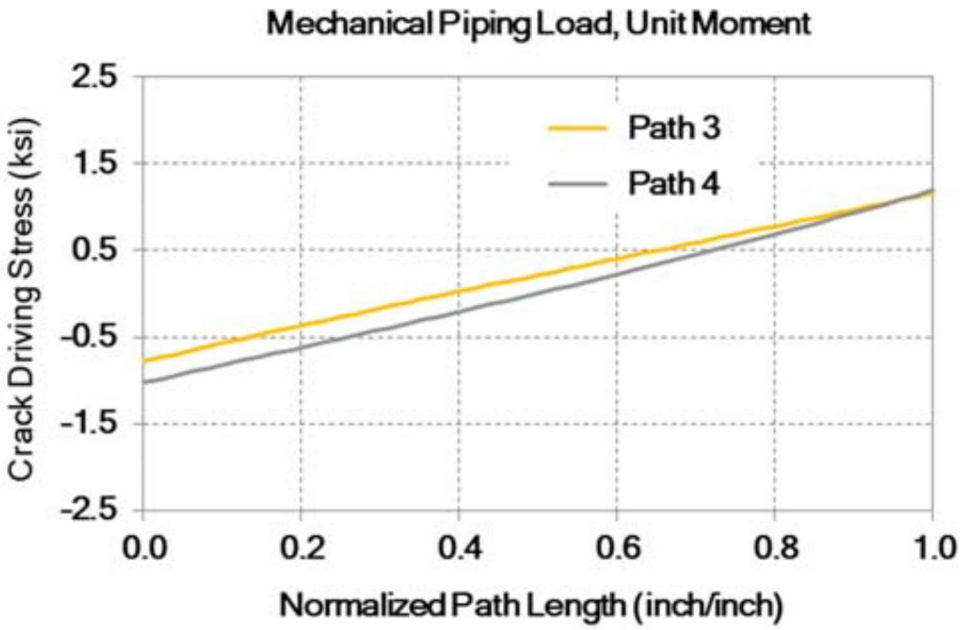

Figure RAI-NVIB-02-C-2: Mechanical Piping Load, Unit Moment Paths P3 and P4

Under the most severe thermal transient (Composite Loss of Feedwater Pumps Event), the stress for P3 is 24 percent larger at the inside diameter as compared to P4, and the difference between the stresses of P3 and P4 decreases as the distance goes to outside diameter.

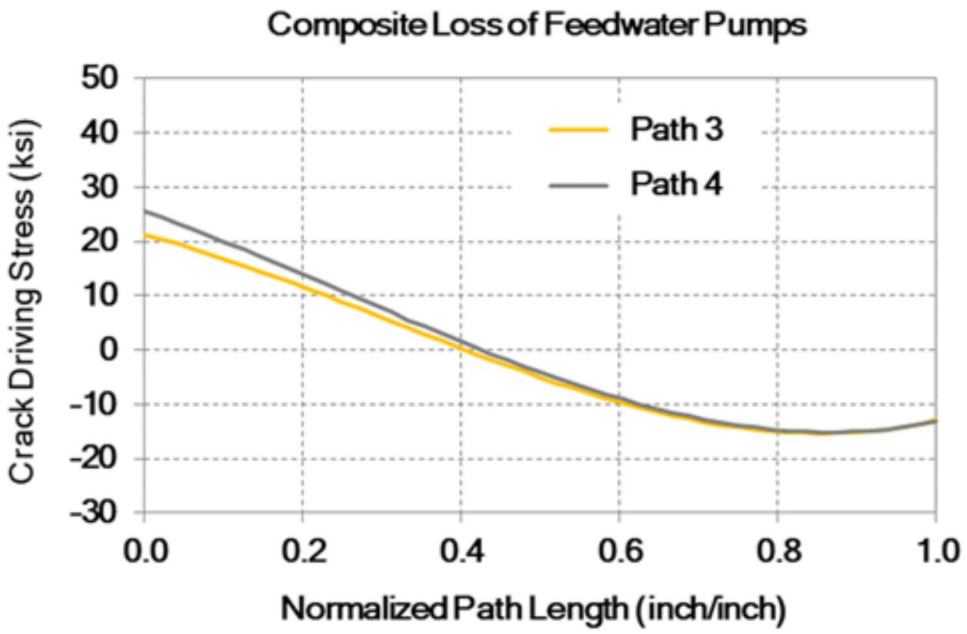

Figure RAI-NVIB-02-C-3: Composite Loss of Feedwater Pumps Paths P3 and P4

Consistent with BWRVIP-108-A and BWRVIP-241-A, the weld residual stress is assumed to be a cosine distribution through the wall thickness with 8 ksi mean amplitude and 5 ksi standard deviation. Because the nozzle-to-vessel welds have cladding, cladding stresses were applied to stress paths P3 and P4 with 32 ksi mean amplitude and 5 ksi standard deviation. The stress distribution of the cladding stress used in VIPERNOZ is in accordance with BWRVIP-05, Section 8.2.3, page 8-8. The same distribution is also used in BWRVIP-108-A and BWRVIP-241-A.

(d) why the past VIPERNOZ Monte Carlo analyses for RFW nozzle-to-vessel welds at CGC, as explained in Energy Northwest RAI response (ML20296A684), ran more stress path assessments for random-generated semi-elliptical axial flaws in the welds. Whereas, presumably the stress path modeling for the corresponding VIPERNOZ Monte Carlo analyses for RFW nozzle-to-vessel welds at PNPP is only modeling one stress path for random generated semi-elliptical axial flaws in welds (i.e., under either stress path (P3 or P4), as applicable to the axial flaw orientation, where the other path (P4 or P3) would be used for the semi-elliptical circumferential flaw analysis runs in the welds).

Response to Part (d):

The methodology follows the precedent from previous ASME Code Case N-702 submittals and BWRVIP-108-A and BWRVIP-241-A, which are the technical basis documents for Code Case N-702. Previous evaluations (most recently for the Brunswick, Units 1 and 2 Recirculation Outlet Nozzle - ADAMS Accession Numbers ML20181A004 and ML21005A010) used four stress paths: two stress paths for nozzle blend radii and two stress paths for the nozzle-to-shell welds. Because of the high stresses at the feedwater nozzle body, primarily due to thermal transient, the CGS evaluation included two additional stress paths in the nozzle body, which resulted in extracting six stress paths in total for the PFM evaluation. The results from the CGS feedwater nozzle PFM evaluation showed that both the nozzle blend radii and the nozzle body have the same probability of failure (PoF): less than 1.67×10^{-8} PoF per year due to normal operation and less than 1.67×10^{-11} PoF per year due to low temperature over pressure (LTOP) event. Based on prior experience with the CGS feedwater nozzle PFM evaluation, the most critical stress paths for the PNPP PFM evaluation were selected, thereby limiting the stress paths to four. Furthermore, in the case of PNPP feedwater nozzles, the nozzle body is not considered as a limiting location because it is bounded by the nozzle blend radii paths due to high pressure stress. Therefore, for the PFM evaluation of PNPP feedwater nozzles, the four stress paths are consistent with the technical basis for Code Case N-702.

(IR-063) RAI-NVIB-03

(a) Identify the 54 effective full power year (EFPY) neutron fluence value and 54 EFPY RT_{NDT} value (or ranges of these values at 54 EFPY) for the assessed RFW nozzle inside radius sections and RFW nozzle-to-vessel welds in the VIPERNOZ runs.

Response to Part (a):

All VIPERNOZ runs conservatively evaluated the 54 EFPY neutron fluence as 1.00×10^{17} n/cm2 for both the RFW inside radius and the nozzle-to-vessel weld locations, as stated in Section 3.3.2 and Table 2 of SIA Calculation Package No. 2001178.302. Conservatively, no neutron attenuation was considered through the depth.

Reference 22 in SIA Calculation Package No. 2001178.302 indicated that the 54 EFPY for the RFW nozzles for 60 years of plant operation is bounded by 1.00×10^{17} n/cm2. The referenced report states that the N6 nozzles peak 54 EFPY neutron fluence is 8.1×10^{16} n/cm2. The N4 nozzles are above the N6 nozzles and therefore bounded by a neutron fluence of 1.00×10^{17} n/cm2.

The plant-specific mean values for 54 EFPY RT_{NDT} are specified in Section 3.3.1 and Table 2 of SIA Calculation Package No. 2001178.302:

Mean Initial RT_{NDT} for the RFW Nozzle-to-Shell Weld = -20°F
Mean Initial RT_{NDT} for the RFW Nozzle Forging = -20°F

The standard deviations for 54 EFPY RT_{NDT} are consistent with BWRVIP-108-A and BWRVIP-241-A, as specified in Section 3.3.1 and Table 2 of SIA Calculation Package No. 2001178.302:

Standard Deviation of Initial RT_{NDT} for the RFW Nozzle-to-Vessel Weld = 13°F
Standard Deviation of Initial RT_{NDT} for the RFW Nozzle Forging = 26.48°F

(b) Identify the RFW metal temperature value (or range of RFW metal temperatures) used for the VIPERNOZ runs of the assessed RFW nozzle inside radius locations and the assessed RFW nozzle-to-vessel weld locations and clarify whether the metal temperature is based on that for the inside surface of the component (e.g., metal temperature of the inside surface of the component cladding for RFW nozzle welds assessed under path P3 and P4 or the metal temperature of the inside ferritic steel surface for assessed RFW inside radius sections under Paths P1 and P2) or the metal temperature at the assessed crack tip of the evaluated component flaw in the VIPERNOZ PFM Monte Carlo run for the assessed RFW nozzle component location. [NOTE: Per the FEM diagrams in IR-063, the RFW nozzle-to-vessel welds have inside cladding layers, but the RFW inside radius sections do not have any clad surface layers. The crack tips of the evaluated flaw types are depicted in the following figures in SIA Calculation No. 2001178.302: (a) Figure A-1 for the semi-elliptical inside surface flaw in the assessed RFW nozzle inside radius section, (b) Figure A-2 for a semi-elliptical, axially-oriented inside surface flaw in the assessed RFW nozzle-to-vessel weld component, and (c) Figure A-3 for a semi-elliptical, circumferentially-oriented inside surface flaw in the assessed RFW nozzle-to-vessel weld component.]

Response to Part (b):

Taking precedent from the response to Request for Additional Information (RAI) 3.4 (ADAMS Accession No. ML20296A684) for the CGS RFW relief request regarding the technical justification of the 200 ksi$\sqrt{in}$ K_{IC} (material fracture toughness) value for the fracture toughness, which was found acceptable by the NRC in Section 3.2.7.2 of the safety evaluation (ADAMS Accession No. ML21096A48), Figure 4 of SIA Calculation Package No. 2001178.302 shows the maximum stresses that occur during the three most severe transients listed in Table 1 of SIA Calculation Package No. 2001178.302 for the feedwater nozzles at PNPP. The highest thermal stresses (38 ksi at the inside surface) occur during Transient 20 (Composite Loss of Feedwater Pumps) at stress

paths P1 and P2. From the stress analyses output files of the two stress paths, the minimum temperature at the inside surface of the component is 365°F at the time of maximum total applied load during Transient 20 (t = 6,250 seconds).

As stated in the response to Part (a) above, the highest initial RT_{NDT} for the RFW is -20°F. The RFW nozzles are remote from the beltline region and therefore the initial RT_{NDT} values do not have to be adjusted for the effects of fluence.

Thus, the minimum (T - RT_{NDT}) during the maximum thermal stresses is conservatively calculated as 365°F – (-20°F) = 385°F.

Per Figure A-4200-1 of ASME Code, Section XI, Appendix A, the value of K_{IC} is 220 ksi√in for 385°F at the time of maximum total applied load for the PNPP RFW. Hence, the lower value of 200 ksi√in used in the evaluation is conservative.

(IR-063) RAI-NVIB-04

(a) Confirm that the SIA VIPERNOZ Monte Carlo flaw growth methods account for OBE [operational basis earthquake] load contributions as part of the "Bounding Group Event" Startup transient contributions to the reiterative VIPERNOZ Monte Carlo fatigue flaw growth runs (that is, as part of the "Startup" transient fatigue contributions to the runs for RFW nozzle inside radius sections and nozzle-to-vessel welds as a result of moments caused by loads applied at the nozzle-to-nozzle safe-ends regions).

Response to Part (a):

For the Monte Carlo flaw growth methods, two separate loading combinations with different ΔK (as described in Part (b)) were used to independently account for the 80 cycles of the OBE event and 260 cycles of the "Startup" transient:

- The 80 cycles of the OBE event were conservatively assumed to occur during an operating transient (that is, the "Startup" transient) versus Steady-State operation. Consequently, the load combination for the OBE event includes the OBE piping load and the maximum stresses from the "Startup" transient applied to both K_{max} and K_{min}.

- In addition to the OBE event using the stresses from the "Startup" transient, a separate loading combination block was applied to the maximum and minimum stresses from the "Startup" transient to account for the 260 cycles of "Startup" transient (that is, the 80 cycles Startup included with OBE are over and above the actual projected Startup cycles).

(b) If the NRC staff's understanding is correct, clarify how any ΔK (i.e., $K_{max} – K_{min}$) contributions from OBE event seismic load cycles are factored into the maximum ΔK assumed for the "Bounding Group Event" Startup transient and how the 80 cycles have been accounted for as a factor of the 260 cycle assumption for the "Bounding Group Event" Startup transient.

Response to Part (b):

Two separate loading combination blocks were used to account for the 80 cycles of OBE event and 260 cycles of the "Startup" transient. The ΔK for the 80 OBE event cycles were applied as the following loading combination block, which includes the maximum stresses from the "Startup" transient:

OBE Event	
K_{max}	K_{min}
$K_{internal\ pressure}$	$K_{internal\ pressure}$
$K_{crack\ face\ pressure}$	$K_{crack\ face\ pressure}$
$K_{deadweight}$	$K_{deadweight}$
$K_{max,\ start\text{-}up}$	$K_{max,\ start\text{-}up}$
$K_{weld\ residual}$	$K_{weld\ residual}$
K_{clad}	K_{clad}
$K_{max,\ OBE}$	$K_{min,\ OBE}$

A separate, independent loading block was applied for the 260 cycles of the "Startup" transient with the following ΔK:

"Startup Event"	
K_{max}	K_{min}
$K_{max,\ internal\ pressure}$	$K_{min,internal\ pressure}$
$K_{max,\ crack\ face\ pressure}$	$K_{min,\ crack\ face\ pressure}$
$K_{deadweight}$	$K_{deadweight}$
$K_{weld\ residual}$	$K_{weld\ residual}$
K_{clad}	K_{clad}
$K_{max,\ start\text{-}up}$	$K_{min,\ start\text{-}up}$

(c) If the NRC staff's understanding is incorrect, explain how the OBE event stresses and cycles are accounted for in the VIPERNOZ Monte Carlo fatigue flaw growth runs for the assessed RFW inside radius sections under load Paths 1 and 2 and for the assessed RFW nozzle-to-vessel welds under Load Paths 3 and 4.

Response to Part (c):

Responses to Parts (a) and (b) above clarifies that the OBE event and “Startup” transient are considered independently with two separate loading combination blocks. This methodology was used for both RFW inside radius sections under load Paths 1 and 2 and for the RFW nozzle-to-vessel welds under load Paths 3 and 4.

(IR-063) RAI-NVIB-05

(a) Confirm that EHNC [Energy Harbor Nuclear Corp.] has not made any weld repairs of the six RFW nozzle-to-vessel welds (or even the RFW nozzle-to-safe end welds) since initial startup of the PNPP reactor unit.

Response to Part (a):

Energy Harbor Nuclear Corp. has not made any weld repairs of the six RFW nozzle-to-vessel welds. Since initial startup of the PNPP reactor unit, Energy Harbor Nuclear Corp. has performed a weld overlay (WOL) repair and applied mechanical stress improvement process (MSIP) on two separate feedwater nozzle-to-safe end welds at PNPP. Nozzle-to-safe end weld 1B13-N4C has a weld overlay. Nozzle-to-safe end weld 1B13-N4E has had a MSIP applied. No other weld repairs have been performed on the six RFW nozzle-to-vessel welds or the RFW nozzle-to-safe end welds since initial startup.

(b) If EHNC has implemented weld repairs in any of the RFW nozzle-to-vessel welds (or nozzle-to-safe end welds) since initial operation of the unit, clarify how stresses introduced by the repair welds were accounted for in the FEM stress analyses for the assessed RFW nozzle-to-vessel weld components (including treatment of any weld residual stresses that may have been introduced into the nozzles as a result of repair welding melt and solidification processes).

Response to Part (b):

The residual stresses resulting from the WOL repair and application of the MSIP treatment at the nozzle-to-safe end weld were not considered in the FEM stress analysis and the PFM evaluation for the nozzle blend radius and the nozzle-to-shell weld in the proposed alternative since the bore blend region is a minimum of 18.508 inches from the areas where the WOL and MSIP were applied. The basis for this conclusion is provided in the following paragraphs.

The WOL and MSIP are intended to provide beneficial compressive stress in welds that are susceptible to stress corrosion cracking (SCC). The concern with performing a WOL or MSIP is if the stress effects induced by the WOL and MSIP carry back to the bore-blend radius region of the nozzle. Since the residual stresses are not cyclic, the

only effect of this compressive stress is on the R-ratio. Compressive R-ratio's slows down crack growth, and so from that viewpoint, it is conservative not to consider them in the crack growth evaluation. However, the WOL includes the additional effect of adding a dissimilar material to the outside surface of the nozzle-to-safe end weld, which can produce stresses that vary with thermal transient cycling and thus impact fatigue crack growth (FCG) behavior.

To determine the impact of the WOL at the bore blend radius, the results from Materials Reliability Program: Technical Basis for Preemptive Weld Overlays for Alloy 82/182 Butt Welds in PWRs (MRP-169), Revision 1, were examined. A RFW nozzle was not specifically evaluated in this document, however, a surge nozzle was examined. The PNPP RFW nozzle outside diameter is 14.25 inches at the nozzle-to-safe end weld and 25.5 inches at the nozzle body. The evaluated surge nozzle diameter is 15 inches at the nozzle-to-safe end weld and 19 inches at the nozzle body. The evaluated surge nozzle is thinner than the RFW nozzle. The increase in material thickness means that the RFW nozzle will be more resilient to stresses and any conclusion reached using the surge nozzle will bound the PNPP RFW nozzle.

Figure RAI-NVIB-05-1, included in this response, is reproduced from MRP-169, Revision 1, Figure 8-12. A review of Figure RAI-NVIB-05-1 shows that at 5 inches from the center of ID repair (located at the nozzle-to-safe end weld):

1. The axial stress at 650°F pre- and post-WOL are compressive and within 3,000 pounds per square inch (psi). And the operating axial stress is a little over 5,000 psi between 650°F pre-WOL and the 650°/2235 pounds per square inch gauge (psig) operating condition. The majority of the operating stress increase will be due to the addition of the pressure loading. Also, note that the RFW nozzle bore blend radius begins 18.09 inches from the center of the nozzle-to-safe end weld, which is 3.618 times further away from where the result shown in Figure RAI-NVIB-05-1. In all cases, the stresses are compressive and compressive stresses decrease the R-ratio, which helps to slow crack growth.

2. Similarly, the hoop stress at 650°F pre- and post-WOL are compressive and within 1,000 psi. The operating hoop stress is a little over 8,000 psi between 650°F pre-WOL and the 650°/2235 psig operating condition. The greater difference between the hoop and the axial operating stress results is largely due to pressure given that the pressure stress will be twice as high as the axial stress. Once again, all of stress results are compressive, which reduces the R-ratio and subsequently crack growth.

Similarly, the residual stress distribution on the inside surface of a surge nozzle due to application of MSIP on the nozzle-to-safe weld is provided in the September 2009 report titled "Evaluation of the Mechanical Stress Improvement Process (MSIP) as a Mitigation Strategy for Primary Water Stress Corrosion Cracking in Pressurized Water Reactors" (ADAMS Accession No. ML092990646). Figure RAI-NVIB-05-2 consists of two graphs and shows the axial and hoop stress distributions (Figures 41 and 45 from the

September 2009 report). As shown in this figure, the residual stresses towards the nozzle are compressive both in the axial and hoop directions, which decrease the R-ratio and slows crack growth.

Based on these results shown in Figures RAI-NVIB-05-1 and RAI-NVIB-05-2 and the discussions above, the residual stresses induced by a WOL or MSIP are potentially compressive at the bore-blend radius stress field, though it's more likely to have dissipated, as would also be the case at the nozzle-to-shell weld. Furthermore, it is also shown that the stresses due to dissimilar material effects of the WOL also would be insignificant at the bore-blend radius. Therefore, not considering the residual stresses resulting from application of WOL or MSIP is conservative relative to PFM results at the nozzle blend radius and the nozzle-to-shell weld of the PNPP RFW nozzles.

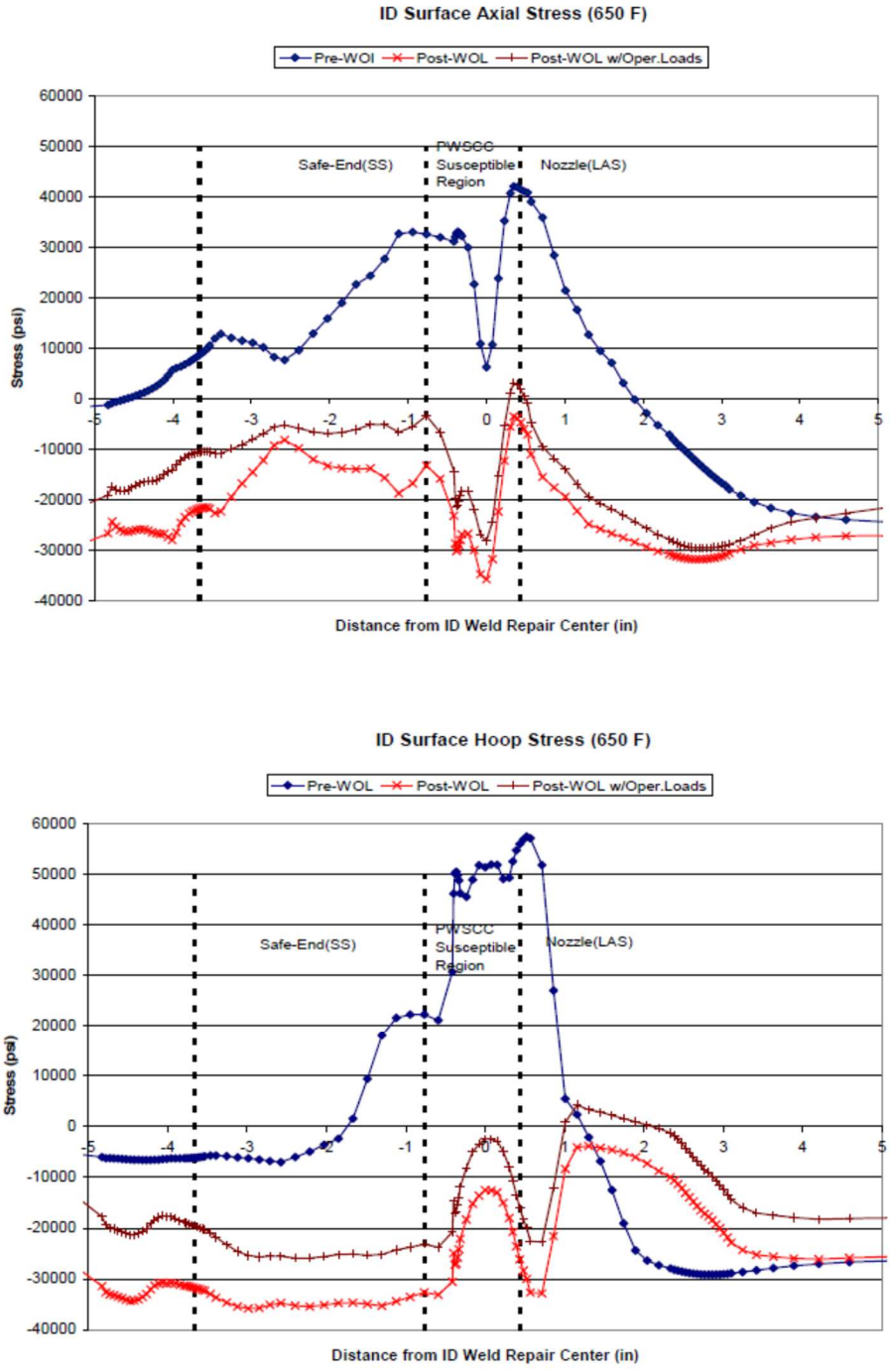

Figure RAI-NVIB-05-1. Pressurizer Surge Nozzle Inside Surface Stress Plots due to WOL Repair

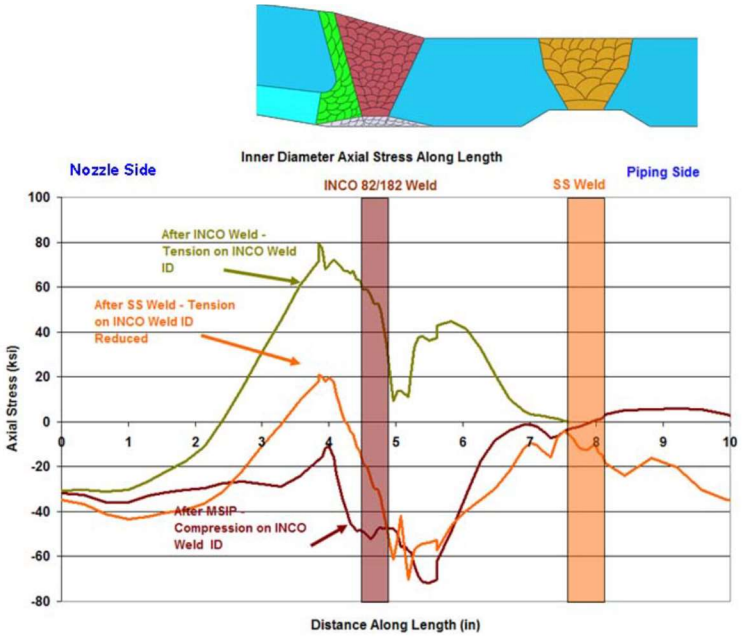

(a) Axial Stress

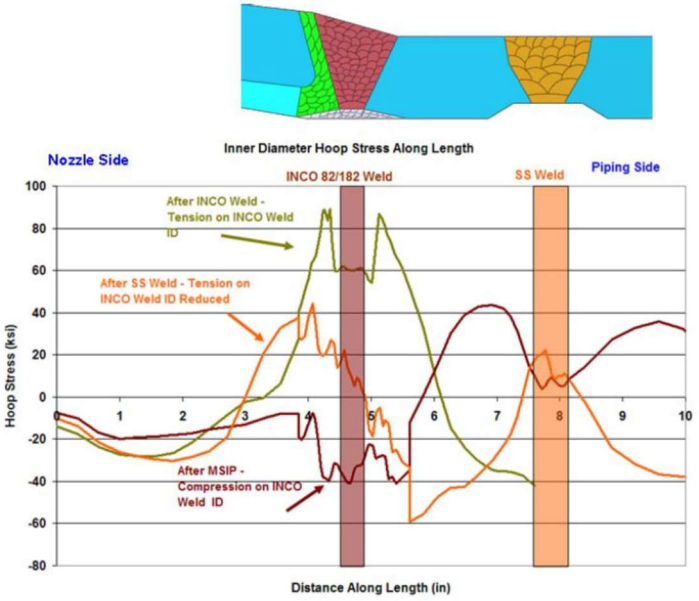

(b) Hoop Stress

Figure RAI-NVIB-05-2. Pressurizer Surge Nozzle Inside Surface Stress Plots due to MSIP

(IR-063) RAI-NVIB-06

(a) Clarify whether the alternative in IR-063 is rounding the number of nozzle weld and nozzle inside radius sections (i.e., required for ISI volumetric inspections) down to one (1) RFW nozzle-to-vessel weld and one (1) RFW nozzle inside radius section during the remainder of the 4th 10-Year ISI interval for the unit or up to two (2) RFW nozzle-to-vessel welds and two (2) RFW nozzle inside radius sections during the remainder of the 4th 10-Year ISI interval for the unit (NOTE: Justification will be needed if rounding down to 1 RFW nozzle-to-vessel weld and 1 RFW nozzle insider radius section).

Response to Part (a):

The alternative described in IR-063 is rounding the number of nozzle weld and nozzle inside radius sections up to two RFW nozzle-to-vessel welds and two RFW nozzle inside radius sections during the remainder of the fourth 10-year ISI interval for the unit.

(b) Clarify whether there are any location-specific considerations that would call for EHNC to pick one or two (depending on the response to Part 1 of this request) of the specified RFW nozzles for the specified inspections over the other RFW nozzles that are included in the population of RFW nozzles in the plant design. If so, explain what the RFW nozzle location-specific considerations are and how they are used to select the specific RFW nozzle(s) that will be inspected during the remainder of the 4th 10-Year ISI Interval for the unit; and identify the specific RFW nozzles (by component ID) that will be inspected during the remainder of the 4th 10-Year ISI Interval as a result of the location-specific considerations.

Response to Part (b):

There are no location-specific considerations that would require Energy Harbor Nuclear Corp. to pick two specific RFW nozzles for the remainder of the fourth 10-year interval. To maximize the use of resources for insulation removal, scaffold builds, and to reduce total dose, the nozzles to be selected in the fourth 10-year interval will be coordinated with the site exams necessary for the nozzle-to-safe end welds.

(IR-063) RAI-NVIB-07

(a) Confirm that for each reiterative VIPERNOZ PFM Monte Carlo method run performed by the PFM methodology (as described in Appendix A of SIA Calculational Pack 2001178.302), the run calculates total flaw growth caused by the applicable stress path for the assessed RFW weld or inside radius section location by: (1) first assessing SCC [stress corrosion cracking] growth in the component location, and (2)

then adding in fatigue growth to the SCC growth to derive the total flaw growth value of the assessed component location.

Response to Part (a):

In the PFM analysis, crack growth is performed incrementally on a yearly basis. On a yearly basis, SCC crack growth is determined first followed by fatigue crack growth. The process is repeated for the whole evaluation period.

(b) Confirm that for each reiterative VIPERNOZ PFM Monte Carlo method run performed by the PFM methodology, the fatigue flaw growth portion of the run includes the following assessment aspects: (1) for fatigue flaw growth determination of grouped "Bounding Group Event" transients assessed in a given Monte Carlo flaw growth run, the run applies the stress intensity range (i.e., ΔK [K_{max} – K_{min}]) for the specific transient in the group with the highest ΔK range and uses the summed, total number of projected 60-year cycles for all transients assessed in the group, and (2) the fatigue flaw growth portion then totals (sums) the fatigue flaw growth contributions from all ten (10) of the evaluated "Bounding Group Event" transients to derive the total fatigue flaw growth contribution to total flaw growth in the Monte Carlo run (i.e., before adding it to the SCC contribution for total flaw growth in the run).

Response to Part (b):

It is confirmed in the VIPERNOZ PFM Monte Carlo simulation that the following methodology is performed in the fatigue crack growth:

1. For the bounding transient event and OBE event listed in Table 1 of the SIA Calculation Package No. 2001178.302, the stress intensity factor range (ΔK) is calculated for each event. Given the number of cycles of each event, the fatigue crack growth is then calculated.

2. After the calculation of the fatigue crack growth of each bounding transient event and OBE event, the contribution of each event to the fatigue crack growth are added to determine the total fatigue crack

(c) Confirm that for each reiterative VIPERNOZ PFM Monte Carlo method run, flaw probability of detection (PoD) and RPV probability of failure (PoD, including PoD for portions of the RPV containing the RFW nozzle appurtenances) are checked in the runs after accounting for total SCC and fatigue induced crack growth for the run.

Response to Part (c):

It is confirmed that in the VIPERNOZ PFM Monte Carlo simulation, the probability of detection (PoD) and probability of failure (PoF, including PoF for portions of the RPV containing the RFW nozzle appurtenances) are checked after the combined crack growth from SCC growth and fatigue crack growth.